Theoretical study of strong-field multiphoton ionization of polyatomic molecules: A new time-dependent Voronoi-cell finite difference method

July 23, 2010

Son, Sang-Kil
CFEL Theory Group, DESY

Overview

- Strong-field phenomena and challenges in numerical simulation
- TDVFD: time-dependent Voronoi-cell finite difference method on multicenter molecular grids
- Orientation-dependent multiphoton ionization of polyatomic molecules including multielectron effects

Strong-field phenomena
&
numerical challenges

Strong-field multiphoton phenomena

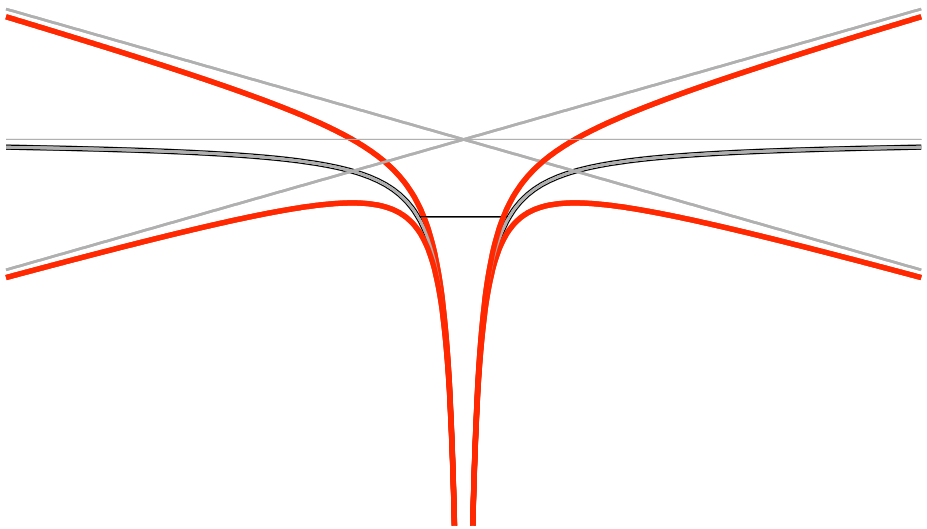

A strong external laser field tilts and oscillates the Coulomb potential.

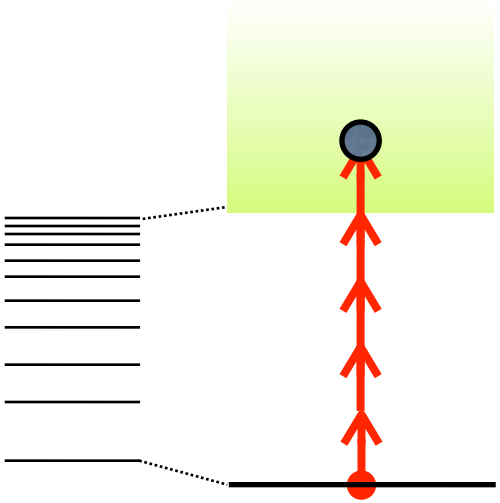

multiphoton excitation / ionization

Multiphoton excitation (MPE), ionization (MPI), and dissociation (MPD), above-threshold ionization (ATI) and dissociation (ATD), multiple high-order harmonic generation (HHG), Coulomb explosion (CE), etc

Molecular alignment

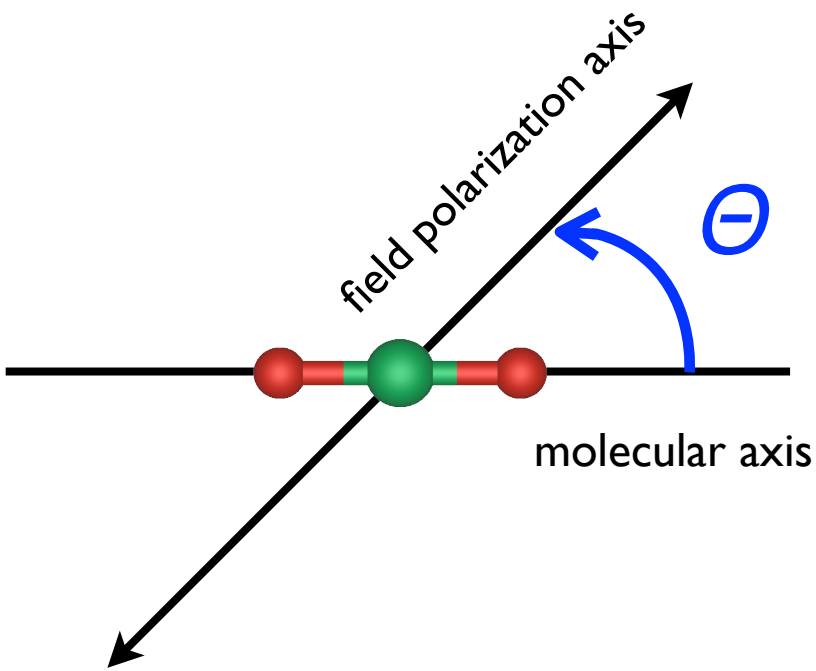

- Laser-induced molecular alignment with an intermediate-intensity laser field
- Probe aligned molecules with a linearly polarized strong laser field
- Measure ionization yields as a function of the orientation angle

Orientation-dependent MPI

820 nm, 1.1×10^{14} W/cm^2

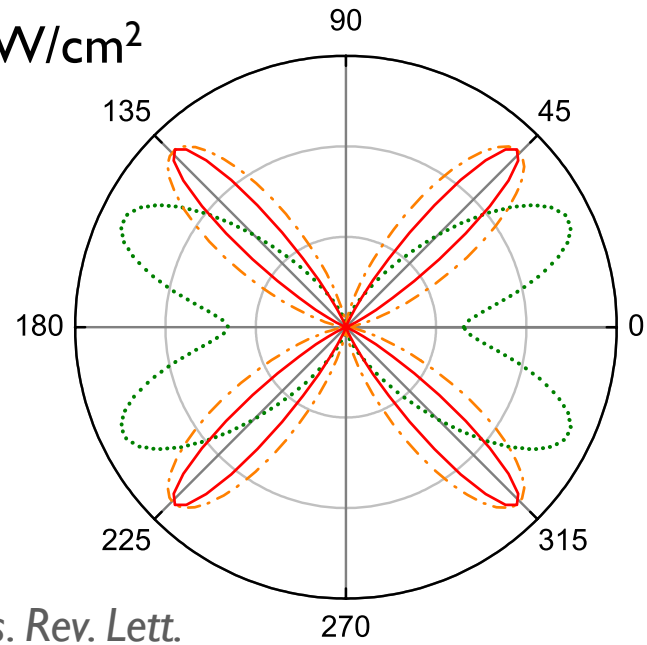

CO_2

Pavičić et al., *Phys. Rev. Lett.* **98**, 243001 (2007)

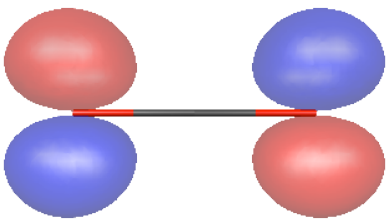

CO_2 HOMO

- Orientation-dependent MPI plot is reflected by the molecular orbital symmetry.
- Most of theoretical models consider only HOMO in many-electron systems.

Numerical simulation for strong-field processes

- Challenges in *ab initio* calculations for strong-field processes
  - electronic structure for bound / continuum states
  - short- and long-range interactions of the Coulomb potential
  - multielectron effect
  - large spatial dimension & efficient time propagator required
- Many theoretical treatments are limited to simple one-electron models without detailed electronic structures.

TDDFT

- Time-dependent Kohn-Sham equations for *N*-electron system in laser fields

$$i\frac{\partial}{\partial t}\psi_{i\sigma}(\mathbf{r},t) = \left[-\frac{1}{2}\boldsymbol{\nabla}^2 + u_{\mathrm{eff},\sigma}(\mathbf{r},t)\right]\psi_{i\sigma}(\mathbf{r},t),$$

$$(i = 1, 2, ..., N_\sigma).$$

$$u_{\mathrm{eff},\sigma}(\mathbf{r},t) = u_{\mathrm{ne}}(\mathbf{r}) + u_{\mathrm{h}}(\mathbf{r},t) + u_{\mathrm{xc},\sigma}(\mathbf{r},t) + \mathbf{F}(t)\cdot\mathbf{r}$$

- TDDFT considers responses in multiple orbital dynamics, which are ignored in most of model calculations based on the single-active electron approximation.

- Self-interaction-correction and proper long-range potential are necessary to investigate strong-field multiphoton processes.

Chu, *J. Chem. Phys.* **123**, 062207 (2005)

Grid method

- Generalized pseudospectral method (GPS) and TDGPS on non-uniform grids developed by Prof. Chu's group

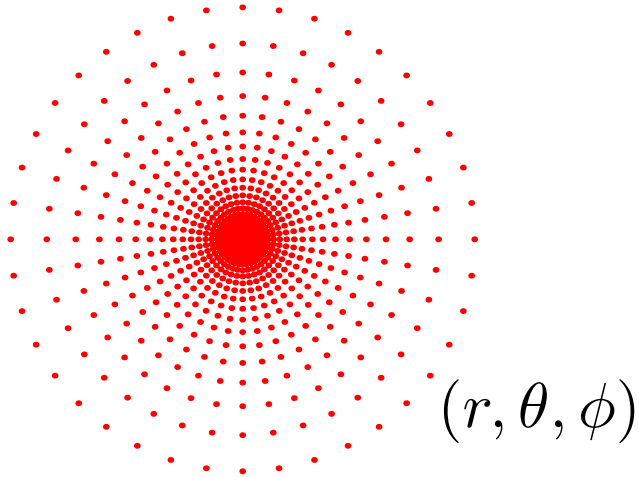

Atoms in the spherical coordinates

Yao & Chu, *Chem. Phys. Lett.* **204**, 381 (1993)

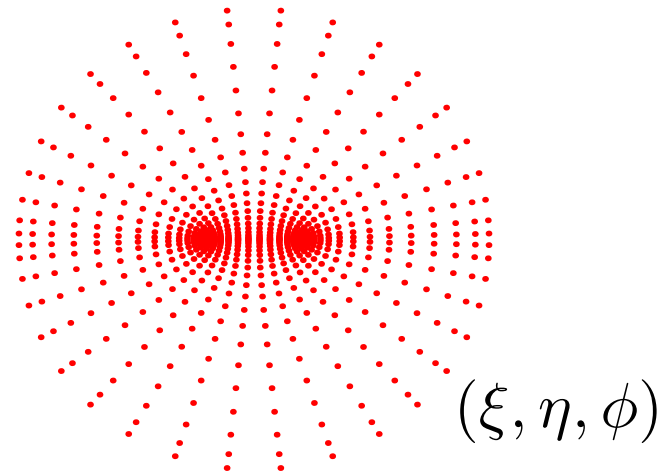

Diatomic molecules in the prolate spheroidal coordinates

Chu & Chu, *Phys. Rev. A* **63**, 013414 (2001)

- Electronic structure: machine accuracy using small # of grids

Beyond atoms and diatomic molecules:
A new method for polyatomic molecules in demand

TDVFD
&
multicenter molecular grids

Voronoi diagram

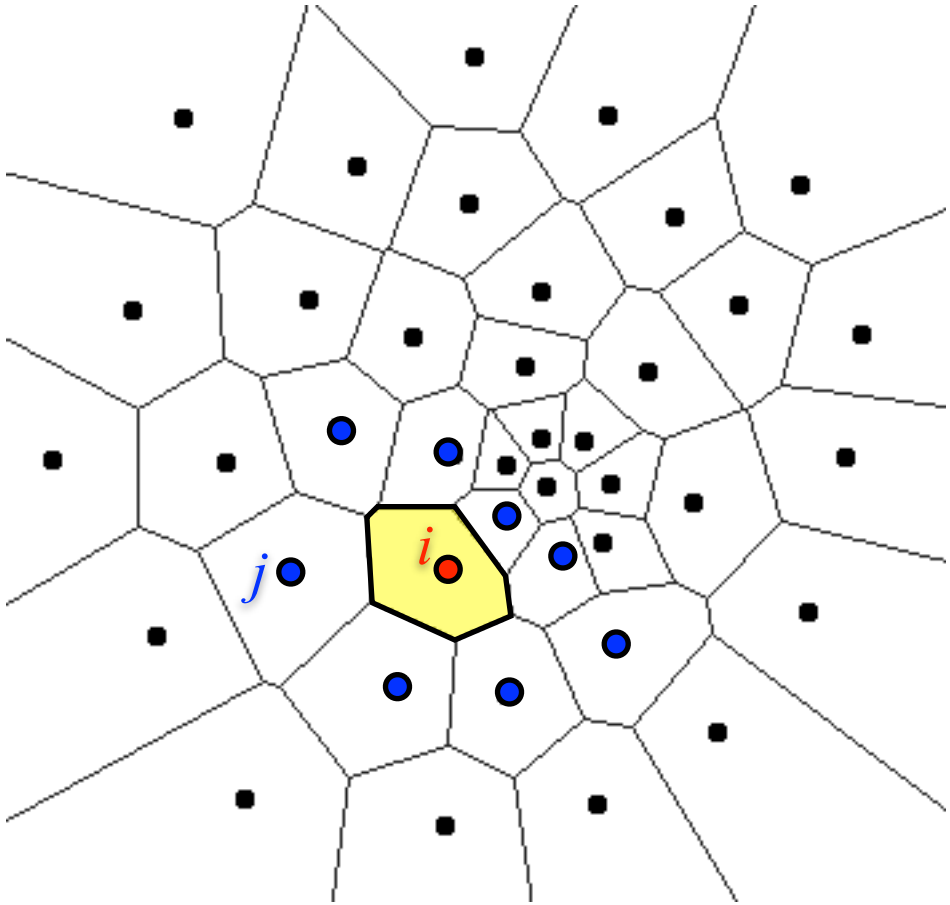

- On randomly distributed grids
- Discretize the whole space into Voronoi cells encapsulating each grid
- PDE solvers utilizing geometrical advantages of the Voronoi diagram

NEM: Braun & Sambridge, *Nature* **376**, 655 (1995)

VFD: Sukumar & Bolander, *CMES* **4**, 691 (2003) / Sukumar, *Int. J. Numer. Meth. Engng* **57**, 1 (2003)

Voronoi diagram: $T_i = \{\mathbf{x} \in \mathbb{R}^n : d(\mathbf{x}, \mathbf{x}_i) < d(\mathbf{x}, \mathbf{x}_j) \text{ for } \forall j \neq i\}$

All points in T_i are closer to $\mathbf{x}_i$ than any other grids.

Voronoi-cell finite difference

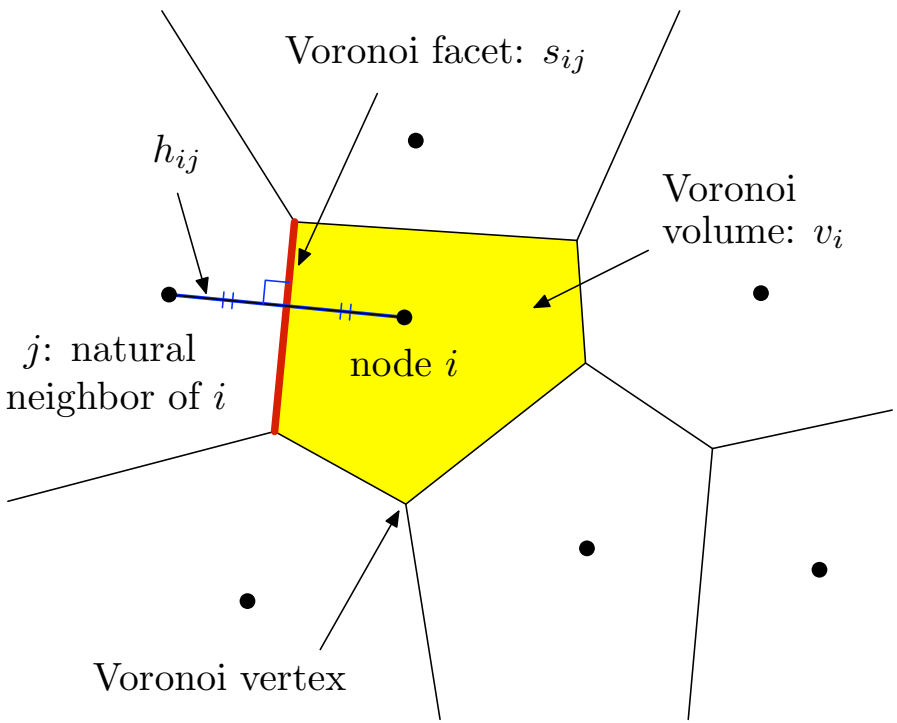

Laplacian definition from Gauss's theorem

$$\nabla^2\varphi = \lim_{\int_V dV \to 0} \frac{\int_S \nabla\varphi \cdot \mathbf{n}\, d\sigma}{\int_V dV}$$

Discrete Laplacian after Voronoi discretization

$$\left(\nabla^2\varphi\right)_i = \frac{1}{v_i} \sum_{j}^{\text{natural neighbors}} \frac{\varphi_j - \varphi_i}{h_{ij}} s_{ij}$$

i) volume and surface integrals are computed by Voronoi volumes and Voronoi facet areas

ii) a simple difference scheme is used for directional derivatives

VFD has been extended for accurate electronic structure and dynamics calculations for the first time.

Son (submitted) / Son & Chu, *Chem. Phys.* **366**, 91 (2009)

Discrete forms in VFD

Laplacian

After symmetrization

$$\tilde{L}_{ij} = \begin{cases} -\dfrac{1}{v_i} \displaystyle\sum_k^{\text{neighbors}} \dfrac{s_{ik}}{h_{ik}} & (i = j) \\ \dfrac{1}{\sqrt{v_i v_j}} \dfrac{s_{ij}}{h_{ij}} & (i,\ j\text{: neighbors}) \\ 0 & (\text{otherwise}) \end{cases}$$

Gradient

From an alternative form of Gauss' theorem

$$G_{ij}^{(x)} = \begin{cases} 0 & (i = j) \\ \dfrac{1}{2v_i} \dfrac{s_{ij}}{h_{ij}} (\mathbf{r}_j - \mathbf{r}_i) \cdot \hat{\mathbf{e}}_x & (i,\ j\text{: neighbors}) \\ 0 & (\text{otherwise}) \end{cases}$$

$G_{ij}^{(y)}$ and $G_{ij}^{(z)}$ are defined likewise.

Integration

Simple nodal quadrature using Voronoi volumes

$$\int_V f(\mathbf{x}) dV \approx \sum_i f(\mathbf{x}_i) v_i$$

Son (submitted) / Son & Chu, *Chem. Phys.* **366**, 91 (2009)

Multicenter molecular grids

1

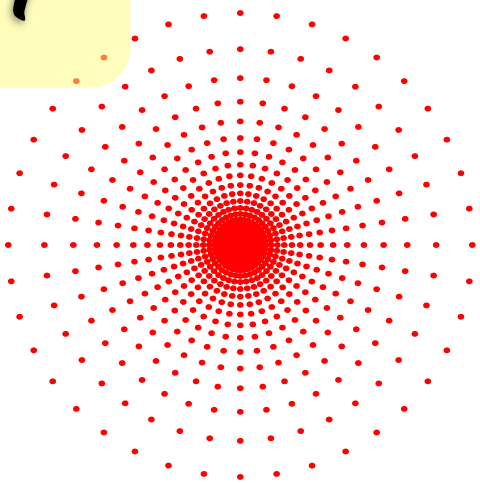

prepare optimal atomic grids

2

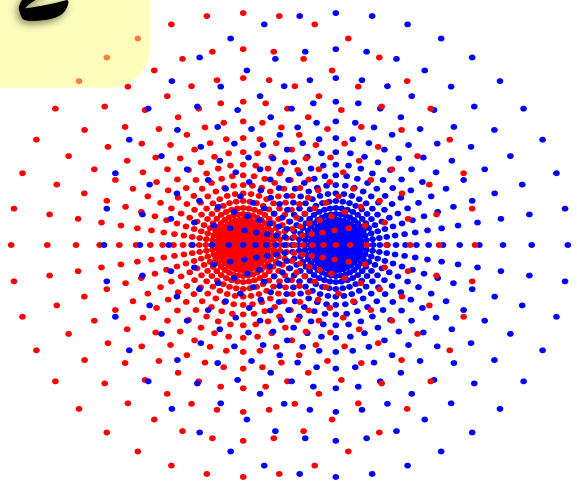

combine atomic grids located at each nuclear position

3

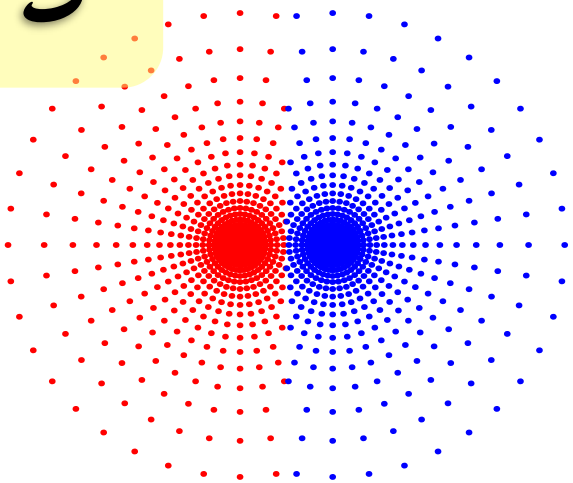

remove overlapped grids (optional)

Molecular grids are intuitively constructed by a combination of spherical atomic grids in 3D.

Molecular grids

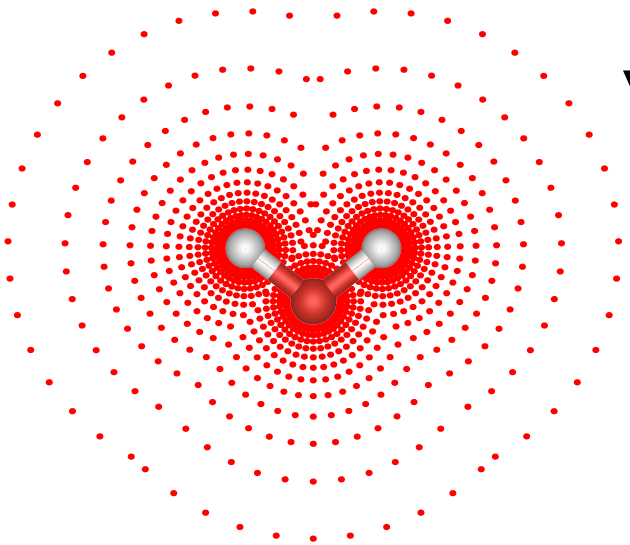

water: H_2O

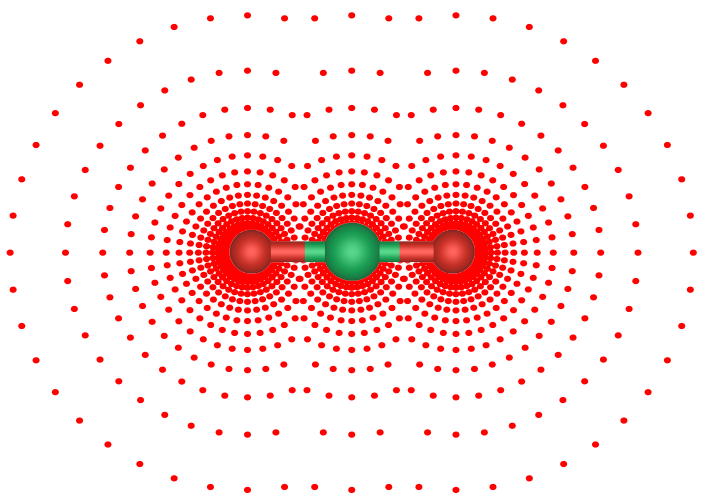

carbon dioxide: CO_2

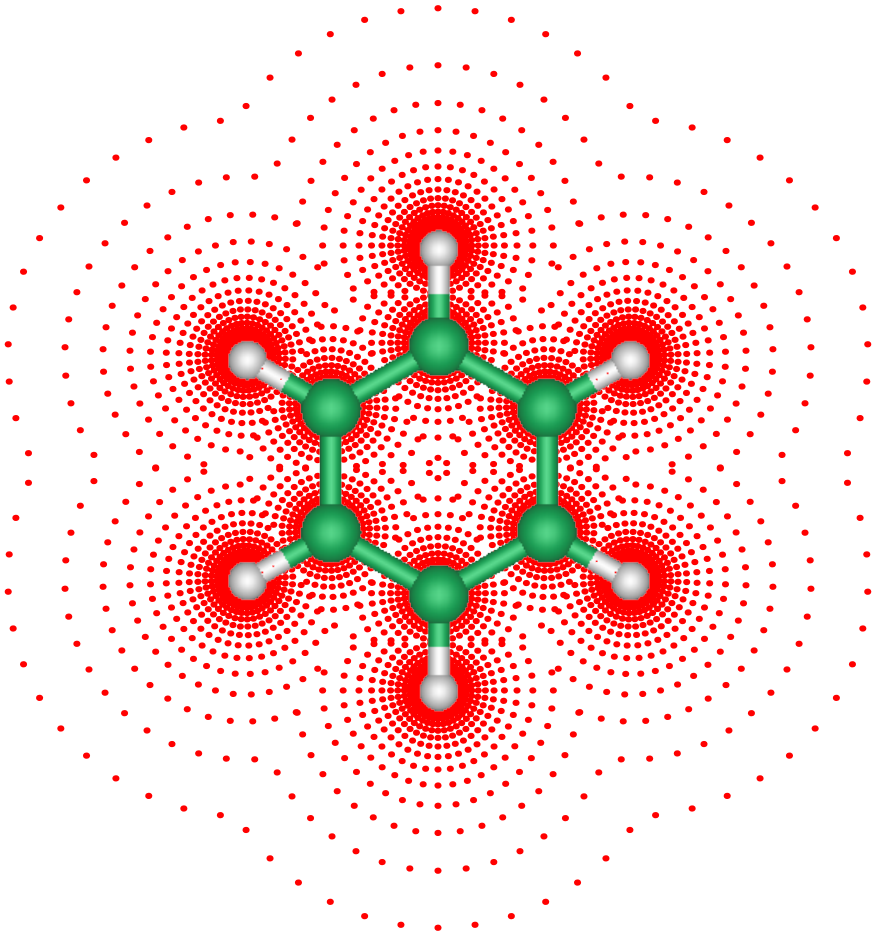

benzene: C_6H_6

VFD works on multicenter molecular grids.

How to resolve Coulomb singularity

$$\tilde{\psi} = r\psi$$

in the spherical coordinates

$$\tilde{\psi} = \sqrt{\xi^2 - \eta^2}\psi$$

in the prolate spheroidal coordinates

$$\tilde{\psi}_i = \sqrt{v_i}\psi_i$$

after the Voronoi discretization

Cusps at the nuclear positions

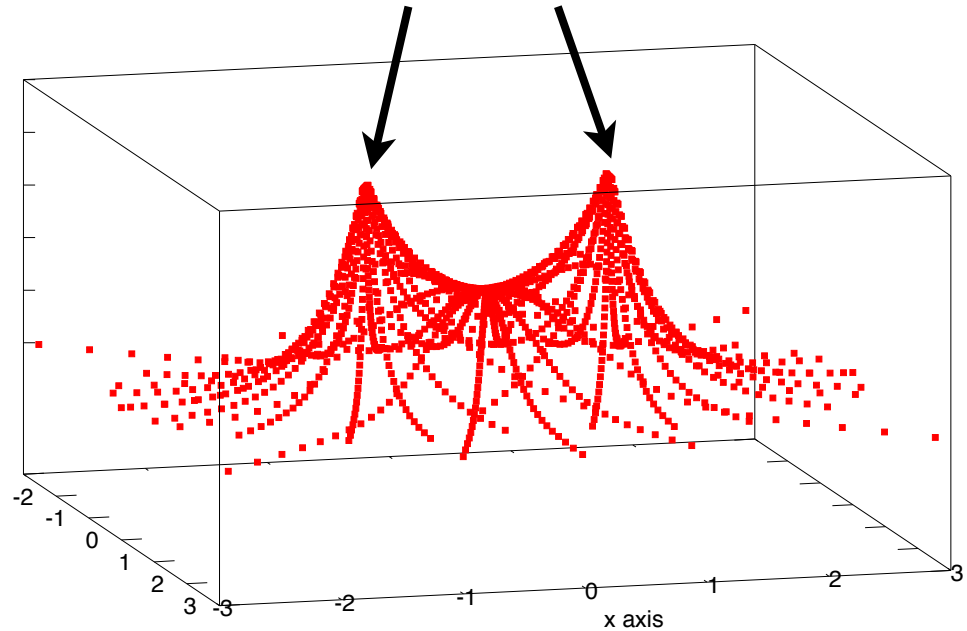

Accuracy assessment

Errors of H_2^+ bound states (one-electron system)

Symmetry	Exact	LCAO–GTO[a]		VFD[b]	
		|error|(a.u.)	|error|(%)	|error|(a.u.)	|error|(%)
$1\sigma_g$	$-1.102\ 634$	1.41×10^{-6}	0.00	4.09×10^{-4}	0.04
$1\sigma_u$	$-0.667\ 534$	1.69×10^{-6}	0.00	5.04×10^{-4}	0.08
$1\pi_u$ (2)	$-0.428\ 772$	1.09×10^{-4}	0.03	2.86×10^{-4}	0.07
$2\sigma_g$	$-0.360\ 865$	5.29×10^{-5}	0.01	2.42×10^{-4}	0.07
$2\sigma_u$	$-0.255\ 413$	2.49×10^{-4}	0.10	2.52×10^{-4}	0.10
$3\sigma_g$	$-0.235\ 778$	3.46×10^{-3}	1.47	3.99×10^{-4}	0.17
$1\pi_g$ (2)	$-0.226\ 700$	4.23×10^{-3}	1.87	5.92×10^{-4}	0.26
$1\delta_g$ (2)	$-0.212\ 733$	5.40×10^{-2}	25.40	8.40×10^{-4}	0.40
$2\pi_u$ (2)	$-0.200\ 865$	6.02×10^{-2}	29.97	3.00×10^{-4}	0.15
$4\sigma_g$	$-0.177\ 681$	1.39×10^{-3}	0.78	2.96×10^{-4}	0.17
$3\sigma_u$	$-0.137\ 313$	6.44×10^{-3}	4.69	3.28×10^{-4}	0.24
$5\sigma_g$	$-0.130\ 792$	3.77×10^{-2}	28.82	3.66×10^{-4}	0.28

[a]Basis set: aug-cc-pV6Z
[b]Grid parameters: N_r=200, L=1, and $l_{\max}$=26

DFT results

LDA energies (in a.u.)

Molecule	Orbital	FD	LCAO	VFD	GPS
N_2	$3\sigma_g$	-0.379	-0.383	-0.383	-0.383
	$1\pi_u$	-0.411	-0.437	-0.438	-0.438
	$2\sigma_u$	-0.543	-0.494	-0.494	-0.493
	$2\sigma_g$	-1.048	-1.039	-1.038	-1.040
	$1\sigma_u$	-14.958	-13.965	-13.971	-13.964
	$1\sigma_g$	-14.959	-13.967	-13.972	-13.966
	E_{total}	-114.100	-108.698	-108.737	
H_2O	$1b_1$	-0.281	-0.272	-0.273	
	$3a_1$	-0.341	-0.346	-0.346	
	$1b_2$	-0.487	-0.488	-0.488	
	$2a_1$	-0.898	-0.926	-0.927	
	$1a_1$	-17.935	-18.610	-18.620	
	E_{total}	-74.286	-75.912	-75.942	

FD: 4th-order FD on uniform equal-spacing grids, Δx=0.1 a.u.
LCAO: aug-cc-pVQZ basis-set
VFD: N_r=300, L=0.5, and $l_{\max}$=32 (Lebedev)

GPS: Chu & Chu, *Phys. Rev. A* **64**, 063404 (2001)

Time propagation

- The split-operator technique in the energy representation

$$\psi(\mathbf{r}, t+\Delta t) = e^{-i\hat{U}(\mathbf{r},t)\frac{\Delta t}{2}}\psi(\mathbf{r},t)e^{-i\hat{H}_0(\mathbf{r})\Delta t}e^{-i\hat{U}(\mathbf{r},t)\frac{\Delta t}{2}}\psi(\mathbf{r},t) + O(\Delta t^3)$$

$$\text{where } \hat{H}_0(\mathbf{r}) = -\tfrac{1}{2}\boldsymbol{\nabla}^2 + u_{\mathrm{eff},\sigma}(\mathbf{r},0),$$

$$\hat{U}(\mathbf{r},t) = \mathbf{F}(t)\cdot\mathbf{r} + \left[u^{\mathrm{LB}\alpha}_{\mathrm{xc},\sigma}(\mathbf{r},t) - u^{\mathrm{LB}\alpha}_{\mathrm{xc},\sigma}(\mathbf{r},0)\right] + \left[u_{\mathrm{h}}(\mathbf{r},t) - u_{\mathrm{h}}(\mathbf{r},0)\right]$$

- $H_0(\mathbf{r})$ is accurately solved within VFD; $\exp[-iH_0(\mathbf{r})\Delta t]$ is solved by the spectral decomposition: $e^{-i\hat{H}_0(\mathbf{r})\Delta t} = \sum_k e^{-i\varepsilon_k\Delta t}|\phi_k\rangle\langle\phi_k|$
- $U(\mathbf{r},t)$ is diagonal in VFD; thus $\exp[-iU(\mathbf{r},t)\Delta t/2]$ is trivial.

Tong & Chu, *PRA* **57**, 452 (1998) / Chu & Chu, *PRA* **63**, 023411 (2001) / Son & Chu, *Chem. Phys.* **366**, 91 (2009)

Orientation dependent MPI of polyatomic molecules

DFT/SIC results

Orbital binding energies (in eV) computed by VFD with experimental (EXP) vertical ionization potentials

Molecule	Orbital	LDA	LBα	EXP
N_2	$3\sigma_g$	10.4	15.5	15.5
	$1\pi_u$	11.9	16.9	16.8
	$2\sigma_u$	13.5	18.5	18.6
	$2\sigma_g$	28.2	33.0	37.3
	$1\sigma_u$	380.1	402.8	409.9
	$1\sigma_g$	380.2	402.8	409.9
H_2O	$1b_1$	7.4	12.5	12.6
	$3a_1$	9.4	14.5	14.8
	$1b_2$	13.3	18.2	18.7
	$2a_1$	25.2	30.1	32.4
	$1a_1$	506.6	531.0	539.7

VFD: N_r=300, L=0.5, r_{max}=20 a.u., and l_{max}=25 (Womersley)
EXP: Siegbahn *et al.*, *ESCA Applied to Free Molecules* (1969) / Ning *et al.*, *Chem. Phys.* **343**, 19 (2008)

Conventional DFT functionals contain spurious self-interaction energy.

Proper long-range potential with self-interaction-correction (SIC)

$$u_{\text{eff}} \sim -\frac{1}{r} \quad \text{as } r \to \infty$$

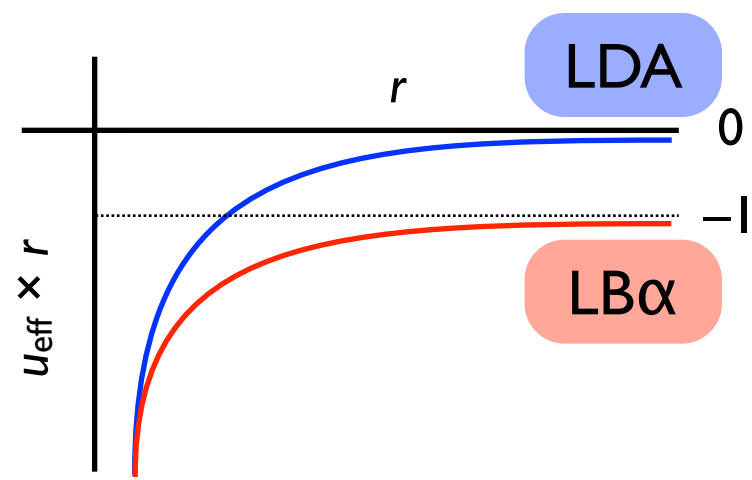

MPI of N_2

Orientation dependence of N_2 MPI
800 nm, 2×10^{14} W/cm^2

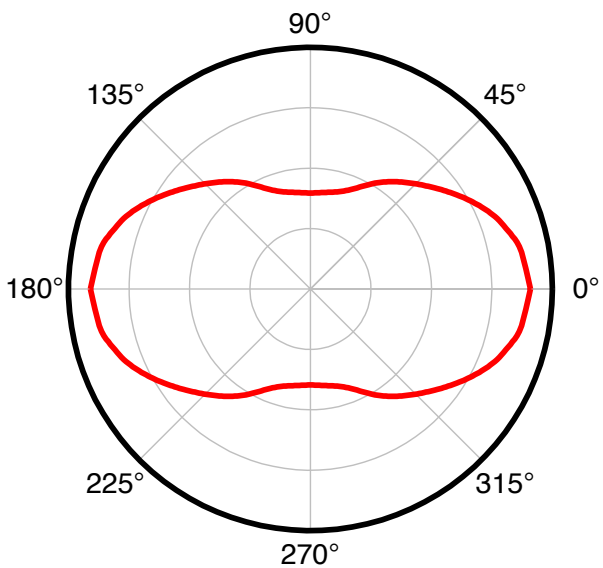

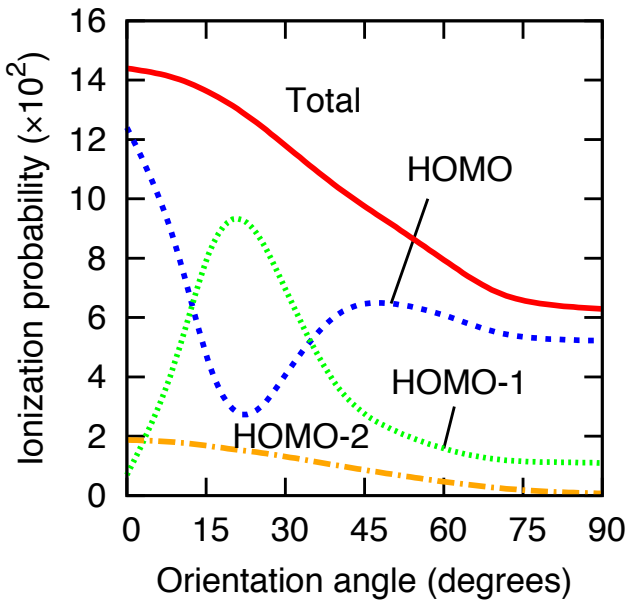

N_2 MO diagram

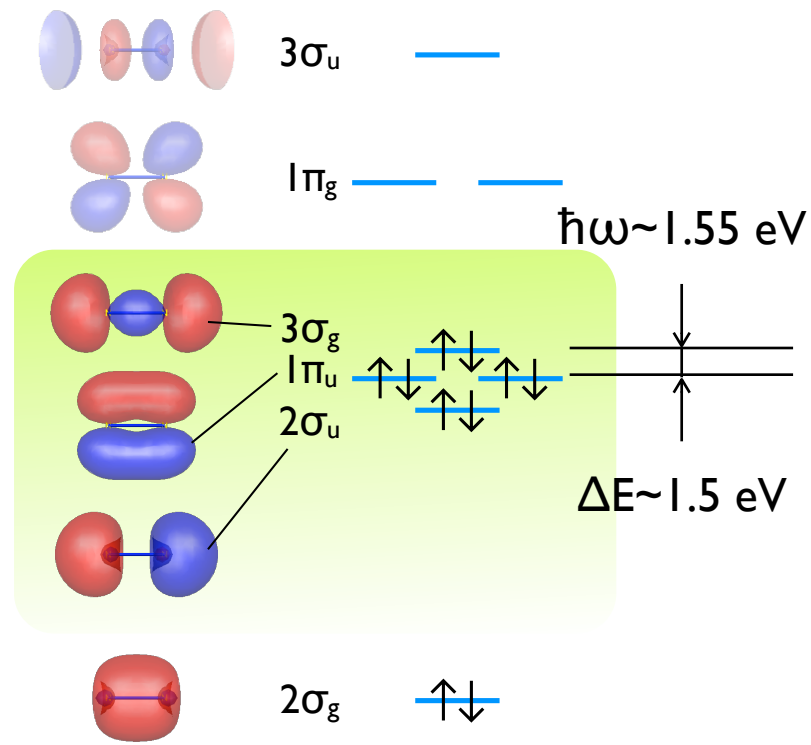

A possible one-photon resonance between HOMO and HOMO–1 yields a strong mixing of their contributions to the total ionization probability.

Son & Chu, *Chem. Phys.* **366**, 91 (2009)

Effects of intensity

N_2 with 800 nm

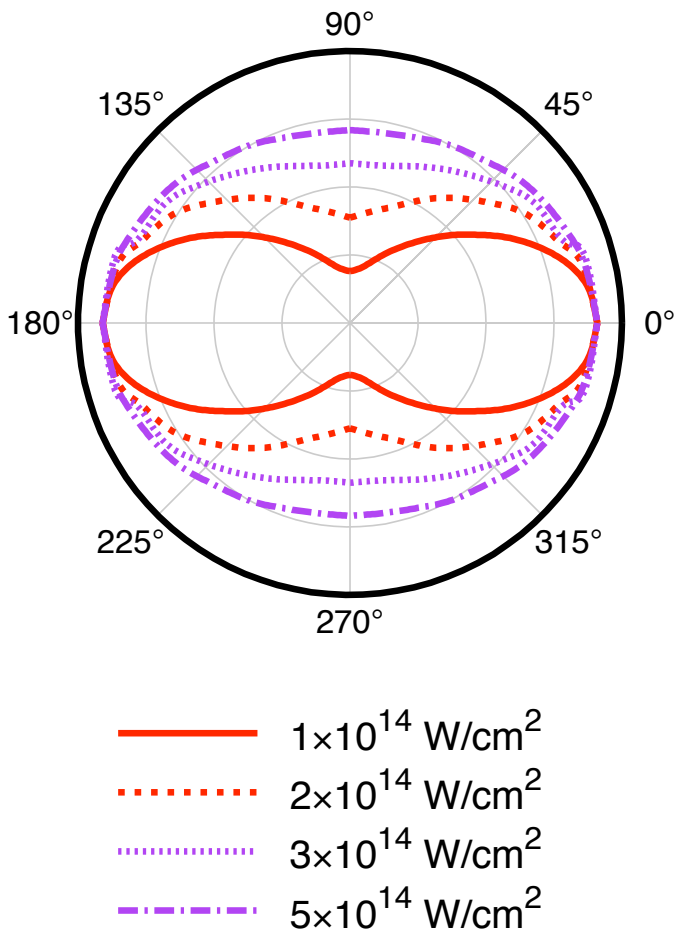

CO_2 with 800 nm

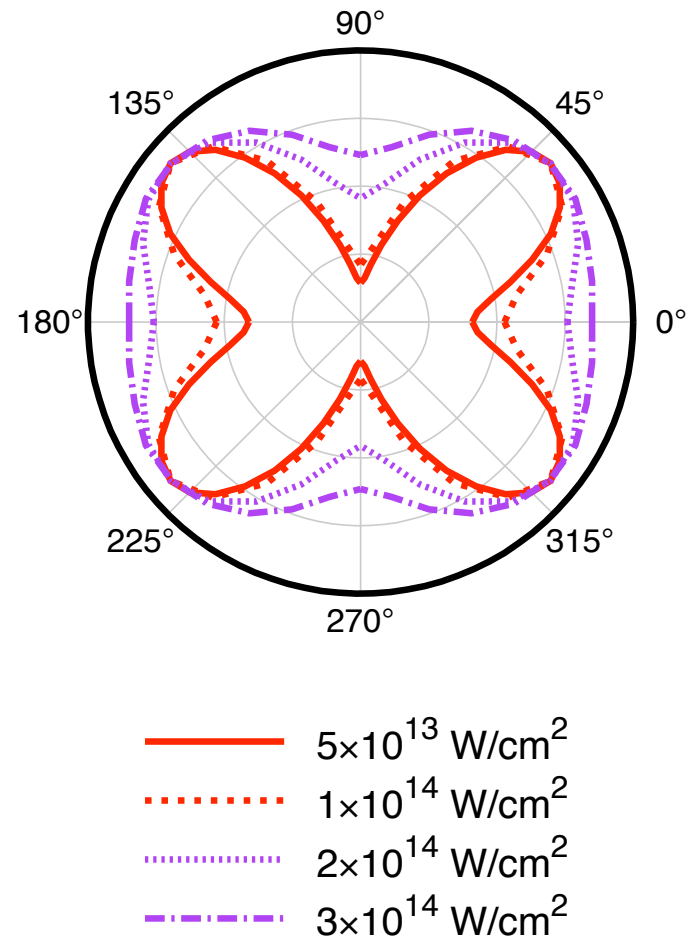

Stronger intensity, less anisotropic

MPI of CO_2

Orientation dependence of total ionization probability

800 nm, 5×10^{13} W/cm^2

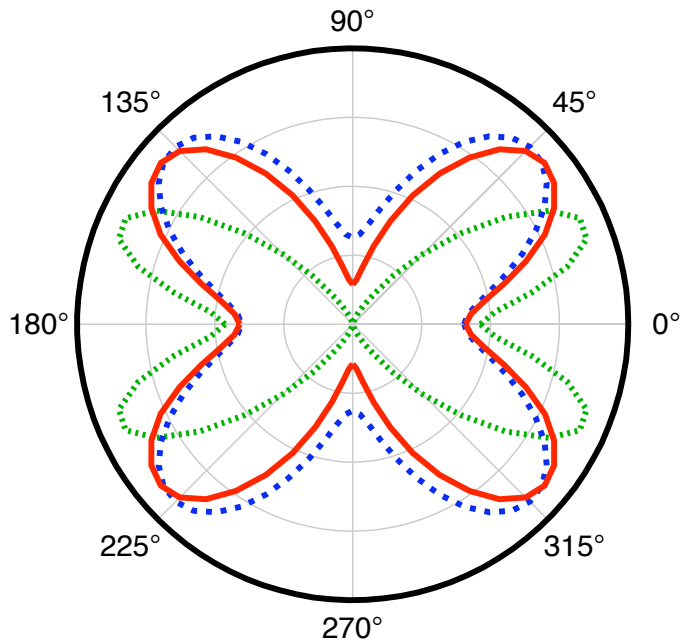

TDDFT: Son & Chu, *Phys. Rev. A* **80**, 011403(R) (2009)

EXP: Thomann *et al.*, *J. Phys. Chem. A* **112**, 9382 (2008)

MO–ADK: Le *et al.*, *J. Mod. Opt.* **54**, 967 (2007)

Orientation dependence of individual ionization probability from multiple orbitals

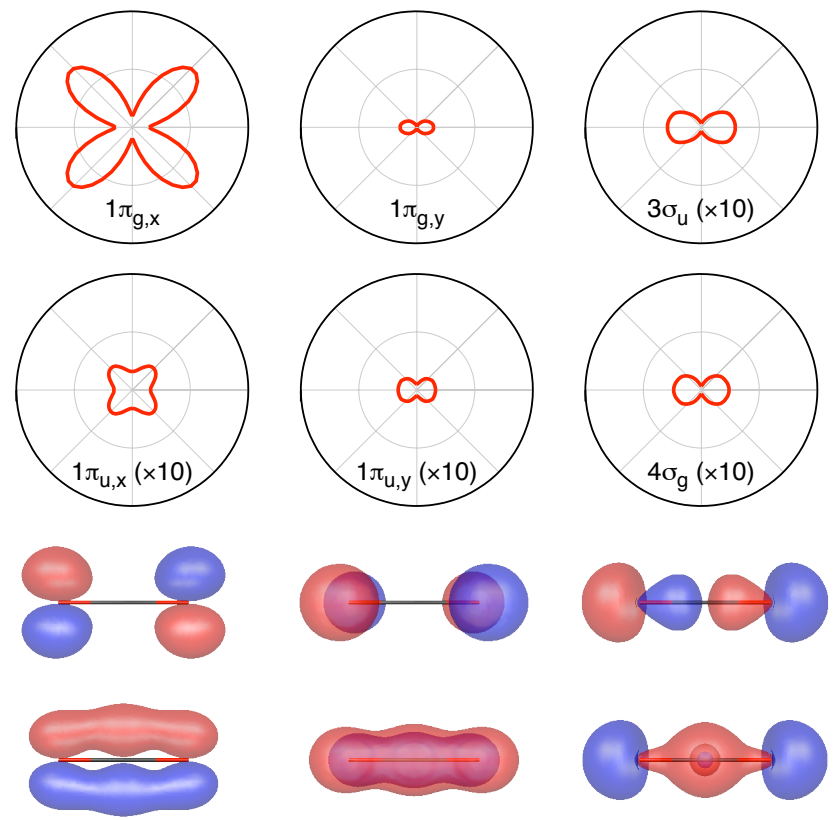

TDDFT results in good agreement with recent experiments

PAD of CO_2

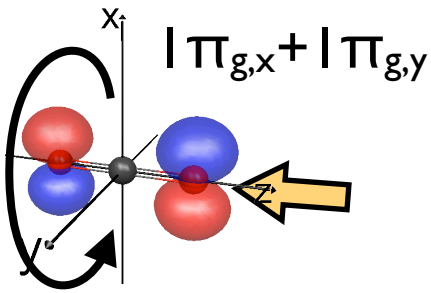

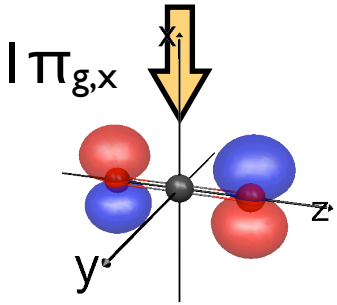

Contour map of $\partial P / \partial \Omega$ on the sphere

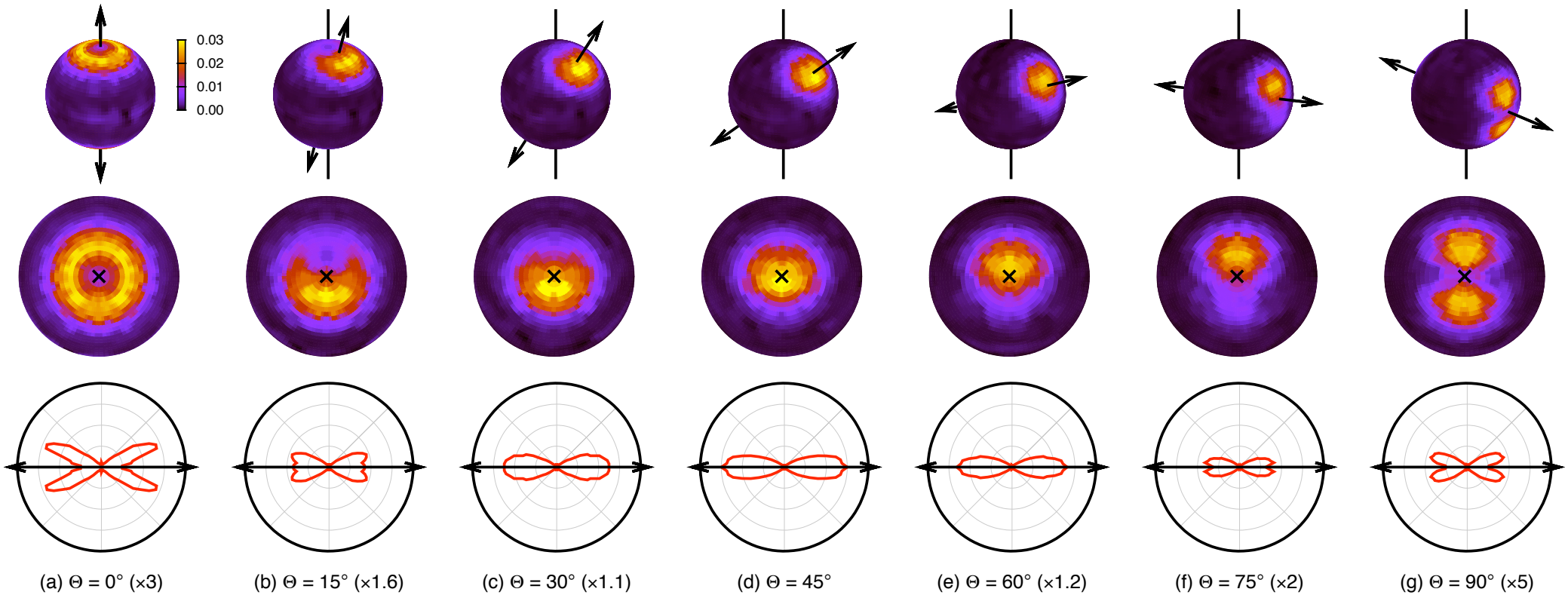

minimum

maximum

minimum

Selectively probing of multiple orbitals in H_2O

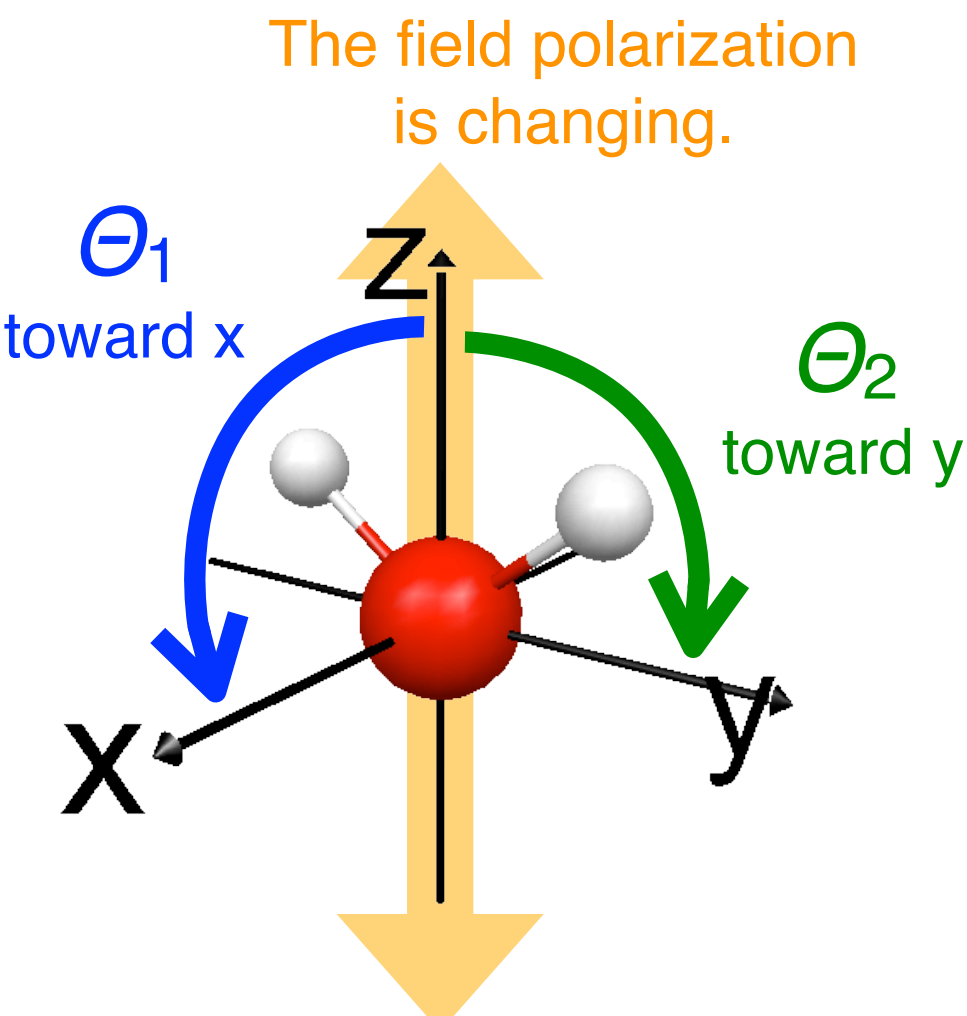

H_2O is contained in the *yz*-plane.

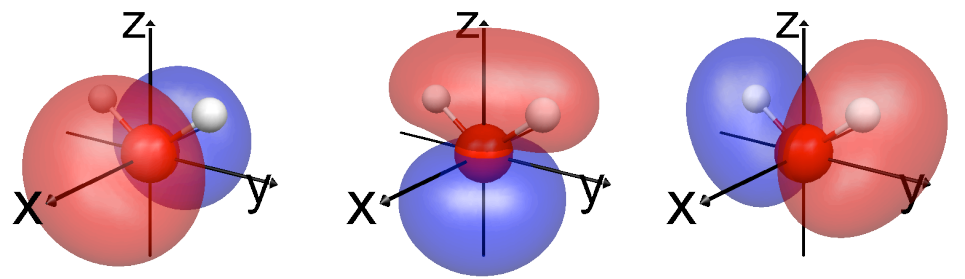

HOMO	HOMO–1	HOMO–2
($1b_1$)	($3a_1$)	($1b_2$)
–12.6 eV	–14.8 eV	–18.7 eV

- Increasing Θ_1 toward x
  - Maximize MPI of HOMO
  - Minimize MPI of HOMO–1
  - No effect on MPI of HOMO–2
- Increasing Θ_2 toward y
  - No effect on MPI of HOMO
  - Minimize MPI of HOMO–1
  - Maximize MPI of HOMO–2

MPI of H_2O

H_2O at 800 nm, 5×10^{13} W/cm^2

orientation-dependent plot w.r.t. Θ_1

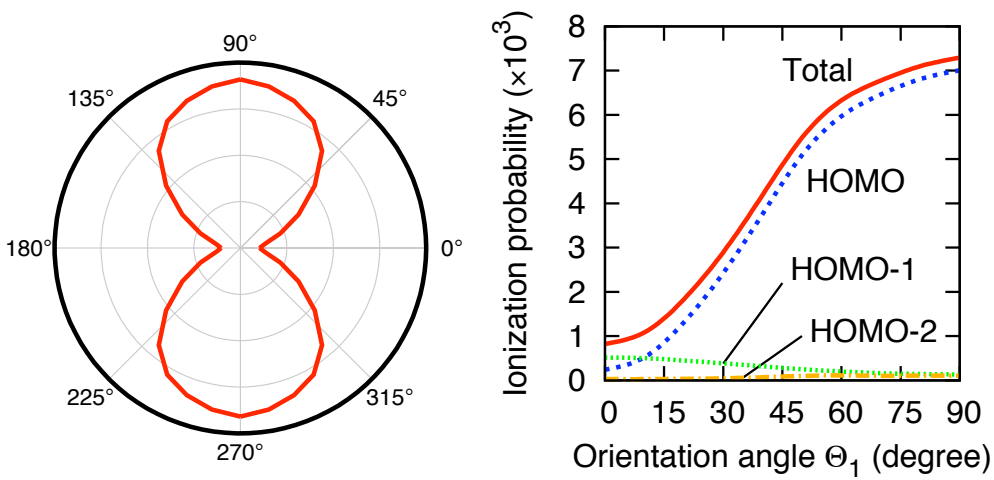

HOMO dominance when Θ_1 changes

H_2O at 800 nm, 5×10^{13} W/cm^2

orientation-dependent plot w.r.t. Θ_2

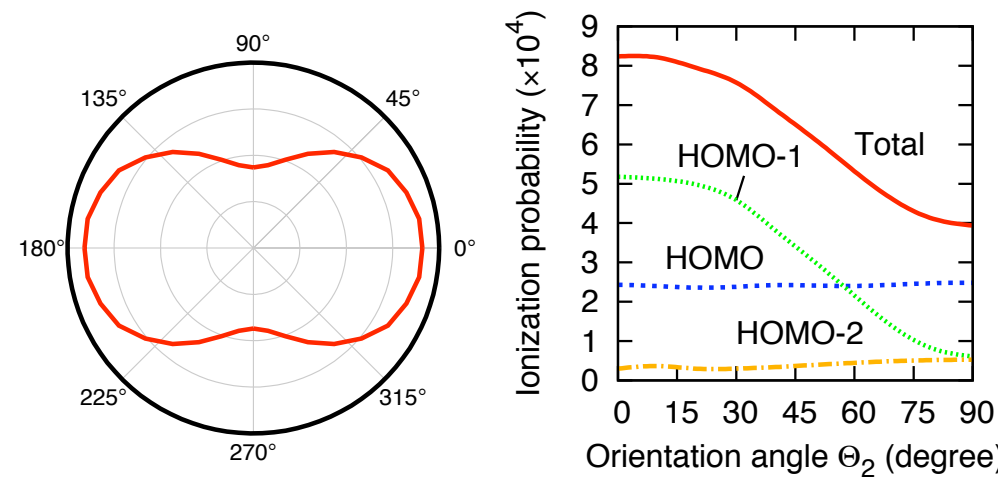

HOMO–1 dominance when Θ_2 changes

First prediction of HOMO–1 dominance in the overall orientation dependence of MPI

Son & Chu, *Chem. Phys.* **366**, 91 (2009)

Conclusion

- VFD is based on Voronoi diagram and natural neighbors: simple like FD / adaptive like FE / formulated like FV.
- TDVFD provides accurate TDDFT solutions for polyatomic molecules on multicenter molecular grids.
- Detailed electronic structure and responses in multiple orbital dynamics are important in strong-field electronic dynamics.
- Orientation-dependent studies of MPI of N_2, H_2O, and CO_2 demonstrate the importance of multielectron effects such as multiple orbital contributions.

Acknowledgment

- University of Kansas
- Prof. Shih-I Chu and colleagues

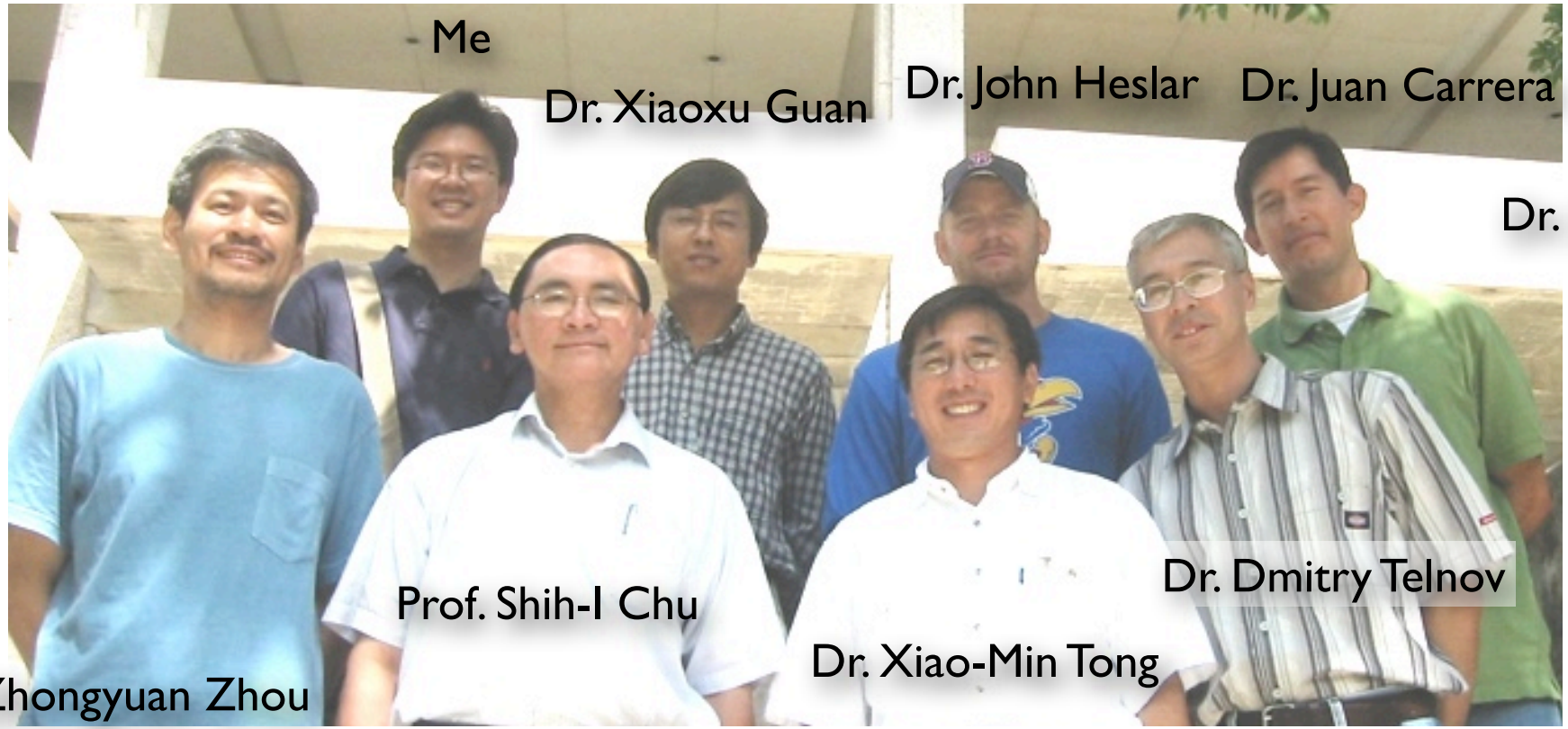


Thank you!